

D3D-VLP: Dynamic 3D Vision-Language-Planning Model for Embodied Grounding and Navigation

Zihan Wang¹ Seungjun Lee¹ Guangzhao Dai² Gim Hee Lee¹

¹School of Computing, National University of Singapore

²Nanjing University of Science and Technology

zihan.wang@u.nus.edu

Abstract

Embodied agents face a critical dilemma that end-to-end models lack interpretability and explicit 3D reasoning, while modular systems ignore cross-component interdependencies and synergies. To bridge this gap, we propose the Dynamic 3D Vision-Language-Planning Model (D3D-VLP). Our model introduces two key innovations: 1) A Dynamic 3D Chain-of-Thought (3D CoT) that unifies planning, grounding, navigation, and question answering within a single 3D-VLM and CoT pipeline; 2) A Synergistic Learning from Fragmented Supervision (SLFS) strategy, which uses a masked autoregressive loss to learn from massive and partially-annotated hybrid data. This allows different CoT components to mutually reinforce and implicitly supervise each other. To this end, we construct a large-scale dataset with 10M hybrid samples from 5K real scans and 20K synthetic scenes that are compatible with online learning methods such as RL and DAgger. Our D3D-VLP achieves state-of-the-art results on multiple benchmarks, including Vision-and-Language Navigation (R2R-CE, REVERIE-CE, NavRAG-CE), Object-goal Navigation (HM3D-OVON), and Task-oriented Sequential Grounding and Navigation (SG3D). Real-world mobile manipulation experiments further validate the effectiveness. The code is available at <https://github.com/MrZihan/D3D-VLP>.

1. Introduction

Effective 3D vision-language grounding [5, 69–71] and navigation [2, 31, 32, 43, 57, 62] are critical capabilities for embodied agents to achieve exploration of large-scale 3D scenes and locate task-relevant objects. However, existing methodologies present a fundamental dilemma. On the one hand, most end-to-end embodied navigation models [12, 56, 59, 64, 65] directly output navigation actions, which bypasses explicit 3D grounding and reasoning processes. However, this simple *black-box* approach impairs

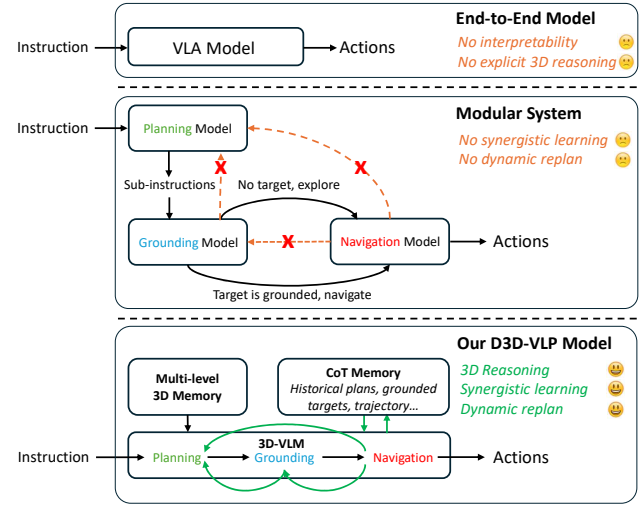


Figure 1. **Model Architecture Comparison.** The end-to-end models directly map instructions to navigation actions, and modular systems assemble multiple specialized components. Our D3D-VLP employs a single 3D-VLM with 3D CoT to unify planning, grounding, and navigation for synergistic learning and planning.

the ability to output precise target locations and introduces limitations for tasks that require long-horizon planning [70] or handling multiple targets. On the other hand, specialized 3D grounding models [10, 11, 22, 26, 76–78] that focus on precise localization often require complete point cloud of the scene or comprehensive RGB-D image sequences as input. This dependence on complete and offline information fundamentally limits their deployment in large-scale, unseen, and dynamic real-world environments [56], where agents must rely on incomplete and real-time observations.

Figure 1 shows some modular systems [6, 36, 37, 39, 52] have achieved commendable performance in their effort to bridge the gap by the integration of Large Language Model (LLM) planners, grounding models, and navigation models. However, these individual components remain essentially disjunct and operating in a multi-stage pipeline. For example, the planner often cannot dynamically update its plan

based on real-time feedback from the grounding and navigation modules. Furthermore, these modules are frequently trained on disparate datasets, creating a significant domain gap that impedes cohesive operation [37].

To address these limitations, we propose the **Dynamic 3D Vision-Language-Planning Model (D3D-VLP)**. As shown in Figure 1 (bottom), our model is designed to bridge the gap between interpretable modular systems and high-performance end-to-end models by introducing two key innovations: **1) Dynamic 3D Chain-of-Thought (3D CoT) Pipeline.** Unlike multi-stage modular systems, our D3D-VLP reformulates planning, grounding, and navigation as a single unified autoregressive task within a 3D-VLM [56]. The *dynamic* nature of our 3D CoT is enabled by a **CoT Memory** feedback loop, which feeds historical plans, grounded targets, and trajectory of the agent back into the context of the model. This mechanism makes the agent stateful and aware of its own progress. It can directly address the static nature of prior planners by performing **dynamic replanning** when a plan is blocked or a target is missing. **2) Synergistic Learning from Fragmented Supervision (SLFS) Strategy.** This strategy trains an unified model without requiring millions of perfectly-annotated samples. Specifically, it allows our D3D-VLP to effectively learn from our 10M-sample hybrid dataset that comprises a small set of *gold* samples and massive quantities of partially-annotated data such as navigation-only. By using a masked autoregressive loss, the gradient from an available annotation such as a correct navigation action back-propagates through the shared 3D-VLM to implicitly supervise and reinforce the internally-generated CoT pipeline of the model. This allows all components to mutually supervise and reinforce each other to achieve **synergistic learning** that is lacking in disjunct modules.

In summary, our main contributions are:

- We propose D3D-VLP, a 3D vision-language-planning model that unifies multi-step planning, grounding, and navigation in unseen and dynamic environments within a single 3D memory and CoT pipeline.
- We introduce the Synergistic Learning from Fragmented Supervision (SLFS) strategy and a supporting 10M-sample large-scale hybrid dataset. This enables our D3D-VLP to learn complex 3D CoT reasoning from massive and partially-annotated sources.
- We demonstrate new state-of-the-art performance with our D3D-VLP across a diverse range of embodied navigation and grounding benchmarks such as R2R-CE, REVERIE-CE, NavRAG-CE, HM3D-OVON, and SG3D, and validate its effectiveness in real-world mobile manipulation experiments.

2. Related Work

3D Visual Grounding. Grounding is a core ability for 3D Vision-Language Models (3D-VLMs) [25, 27, 33, 44, 72, 76–78]. These approaches vary by input modality, where some encode full-scene point clouds [10, 24, 27, 77, 78] while others process object-level segments [21], or aggregate multi-view 2D features into 3D representations [72, 74, 76]. These methods are primarily designed for offline analysis with the assumption of an available complete and static 3D scene. This makes them less directly applicable for embodied agents in unseen, partially observable or dynamic real-world environments.

Embodied Navigation. Recent works [12, 59, 64, 65, 73, 75] show notable performance improvements by using end-to-end large models that directly map instruction and streaming video into navigation actions. Although effective for trajectory following, these approaches often bypass explicit 3D grounding and multi-step planning processes, such grounding-blind design limits their applicability in tasks requiring precise target grounding. Some methods often lack explicit 3D grounding or CoT pipeline [58] for long-horizon planning and multi-target tasks despite their use of 3D-VLMs [56] for navigation.

Modular Planning Systems. To handle long-horizon tasks [47, 48, 70], many systems adopt a modular architecture [6, 13, 39, 52] in which LLMs are often used as high-level planners. These frameworks typically operate in a multi-stage pipeline, where an LLM decomposes the task, a grounding module identifies targets, and a navigation policy executes low-level actions. However, a disjoint architecture hampers dynamic plan updates from real-time feedback. It also leaves domain gaps between modules that are trained on disparate datasets.

Embodied Chain-of-Thought (CoT). Recent works explore integrating Chain-of-Thought (CoT) [58] reasoning into embodied agent, but often without deep 3D grounding and reasoning. NavCoT [34] proposes a text-based navigational chain-of-thought that hallucinates the future observation instead of grounding in the actual observed 3D environment. Embodied CoT [63] grounds 2D bounding boxes and reason with 2D visual features, which is tied to the immediate 2D observation instead of persistent 3D representations. Some models such as SceneCoT [35] attempt explicit 3D grounding and resemble multiple disparate modules without a unified CoT model.

3. Our Method

Overview. Figure 2 shows the framework of our D3D-VLP, a unified 3d vision-language-planning model that integrates planning, grounding, and navigation. At each timestep, we use the encoder of Dynam3D [56] to process streaming posed RGB-D images to update a dynamic Multi-level 3D

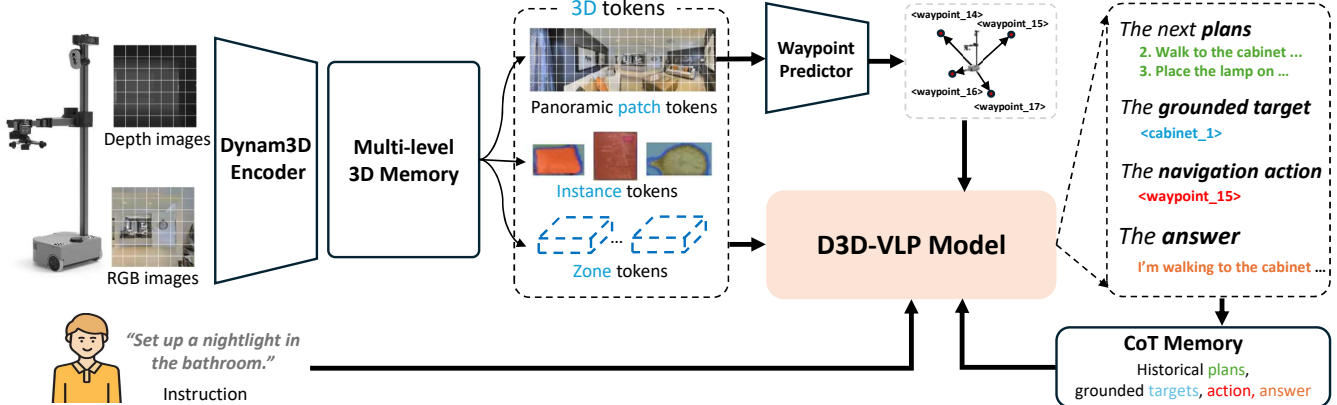


Figure 2. **Framework of our D3D-VLP model.** Given an instruction and streaming posed RGB-D images, a Dynam3D Encoder [56] builds and updates a Multi-level 3D Memory. This memory provides structured 3D tokens (*i.e.* panoramic patch, instance, and zone tokens) to the core D3D-VLP model and a Waypoint Predictor. Our D3D-VLP model then integrates these 3D tokens, the instruction, candidate waypoints, and historical context from the CoT Memory to autoregressively generate a unified 3D Chain-of-Thought (CoT) sequence, which includes the next plans, the grounded target, and the navigation action. Finally, this output updates the CoT Memory to create a dynamic feedback loop for stateful reasoning and replanning.

Memory. This memory provides structured 3D tokens to the pre-trained waypoint predictor and the 3D-VLM. The waypoint predictor would provide several candidate waypoints around the agent. As shown in Figure 3, the 3D-VLM receives the instruction and consults its historical CoT memory. It then autoregressively generates a unified token sequence, including planning text, grounded 3D tokens, the selected next waypoint, and answer text. The updated CoT Memory creates a dynamic feedback loop for replanning and the next decision step.

3.1. Multi-level 3D Perception

The 3D CoT is the reasoning core of our D3D-VLP, which requires a persistent and structured representation of the 3D world. To this end, we employ a foundational 3D perception model [56] that processes streaming posed RGB-D images and maintains a multi-level 3D memory. A waypoint predictor then proposes navigable candidate waypoints.

Dynamic 3D Tokens. The Dynam3D encoder [56] builds a hierarchical scene representation by first projecting 2D patch features into the 3D space, and then encoding the resulting 3D feature points with rich semantic and geometric information. These 3D feature points ($\mathcal{M}_{\text{patch}}$) are then aggregated using transformer-based encoders into object-centric **Instance Tokens** ($\mathcal{M}_{\text{inst}}$) and coarse-grained spatial **Zone Tokens** ($\mathcal{M}_{\text{zone}}$). Furthermore, given the current camera pose, we render **Panoramic Patch Tokens** ($\mathcal{V}_{\text{patch}}$) from 3D feature points ($\mathcal{M}_{\text{patch}}$) using generalizable feature fields [53]. This provides local fine-grained 3D perception following Dynam3D [56]. This structured multi-level 3D representations $\mathcal{M}_t = (\mathcal{V}_{\text{patch}}, \mathcal{M}_{\text{inst}}, \mathcal{M}_{\text{zone}})$ provides the rich and hierarchical 3D visual context that our 3D-VLM (*cf.* Section 3.2) requires for its unified reasoning process.

Waypoint-based Action Space. We train a waypoint predictor instead of following prior works in using text-based actions such as “move forward 0.5m” or “turn left 15 degrees” to simplify the action space and align the spatial semantics between navigation actions and multi-level 3D tokens. Similar to [23], this waypoint predictor inputs panoramic patch tokens ($\mathcal{V}_{\text{patch}}$) and 12 query tokens (spaced 30° apart) into a multi-layer transformer to output nearby navigable locations.

Unified 3D Spacial Embedding. For the multi-level 3D tokens and waypoints, we employ a unified 3D spatial embedding to align their spatial semantics. Specifically, for each timestep t , we transform the global coordinates of the 3D tokens into the agent-centric camera coordinate system using the current camera pose to get $P_t = (P_{\text{patch}}, P_{\text{inst}}, P_{\text{zone}})$. Similarly, we obtain the waypoint coordinates P_{wayp} . For each 3D coordinate point $P_t = (x_t, y_t, z_t)$, the relative distance D_t and the relative horizontal angle θ_t to the agent can be easily calculated. Subsequently, we get the corresponding spatial embeddings \mathcal{P}_t by feeding $(P_t, D_t, \cos(\theta_t), \sin(\theta_t))$ into an MLP-based spatial_encoder(\cdot).

3.2. Dynamic 3D Chain-of-Thought (3D CoT)

The core of our agent is the 3D-VLM (*cf.* Figures 2-3), which directly addresses the *disjunct* and the *no synergistic learning* limitations of modular systems (*cf.* Figure 1). This is achieved by reformulating the entire embodied task from high-level task decomposition (planning) and object localization (grounding) to low-level action (navigation) as a single and unified autoregressive generation problem.

Unified Autoregressive Formulation. The 3D-VLM is implemented as an autoregressive multimodal model loaded

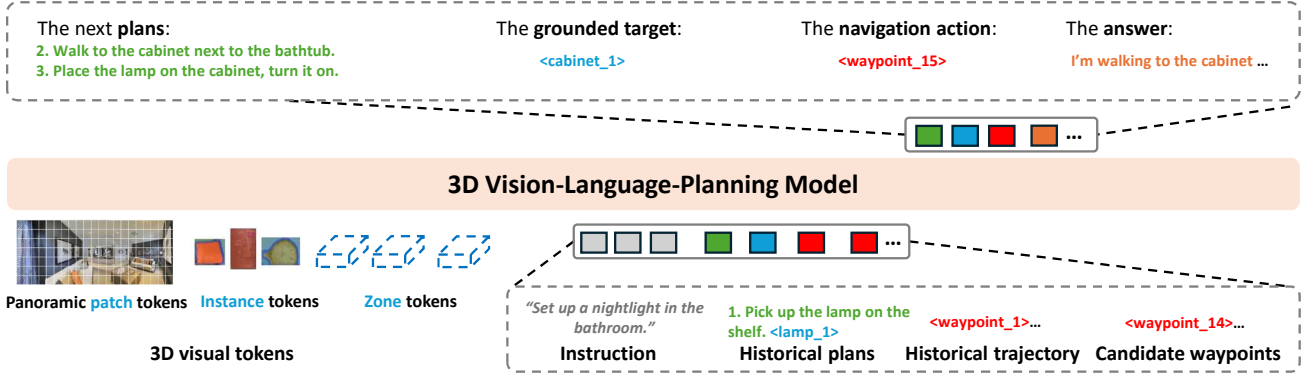


Figure 3. **The Unified Autoregressive Formulation of our D3D-VLP model.** The core 3D Vision-Language-Planning model takes a comprehensive set of inputs: the natural language instruction, multi-level 3D visual tokens (*i.e.* panoramic, instance, and zone), candidate waypoints, and the historical CoT Memory (including past plans and trajectory). It then autoregressively generates a single and unified 3D Chain-of-Thought (CoT) sequence. This multimodal output stream explicitly contains the next plans, the grounded target, the selected navigation action, and a natural language answer.

from a pre-trained NVILA-Lite-2B [38]. At each timestep t , it takes a comprehensive context as input:

- a) The **Multi-level 3D Representations** $\mathcal{M}_t \oplus \mathcal{P}_t = (\mathcal{V}_{\text{patch}}, \mathcal{M}_{\text{inst}}, \mathcal{M}_{\text{zone}}) \oplus (\mathcal{P}_{\text{patch}}, \mathcal{P}_{\text{inst}}, \mathcal{P}_{\text{zone}})$. Similar to Dynam3D [56], these 3D tokens are projected into the the latent space of the VLM, *i.e.* NVILA-Lite-2B [38] with a MLP-based projector(\cdot) through contrastive learning.
- b) The **Instruction** text tokens \mathcal{I} .
- c) The historical **CoT Memory** \mathcal{C}_{t-1} from the previous timestep, as described later in Paragraph **CoT Memory[†]**.
- d) The candidate waypoints embeddings $\mathcal{P}_{\text{wayp}}$.

The 3D-VLM is then trained to autoregressively generate a single coherent sequence \mathcal{S}_t that represents its complete chain-of-thought:

$$p(\mathcal{S}_t \mid \mathcal{I}, \mathcal{M}_t \oplus \mathcal{P}_t, \mathcal{C}_{t-1}). \quad (1)$$

As illustrated in Figure 3, this output sequence \mathcal{S}_t is a structured concatenation of multimodal tokens $\mathcal{S}_t = (\mathcal{T}_{\text{plan}}, \mathcal{T}_{\text{ground}}, \mathcal{T}_{\text{nav}}, \mathcal{T}_{\text{answer}})$:

- a) $\mathcal{T}_{\text{plan}}$: A sequence of natural language tokens representing the next step(s) of the high-level plan, *e.g.* “The next plans: 2. Walk to the cabinet next to the bathtub. 3. Place the lamp on the cabinet, turn it on”.
- b) $\mathcal{T}_{\text{ground}}$: This sequence is not only language generation. Instead, the model outputs multimodal tokens: “The grounded: target<target_1>, target<target_2>”. These special tokens (*e.g.* <target_1>) are autoregressively followed by the word “target” and points to the corresponding 3D tokens from the \mathcal{M}_t (*e.g.* <cabinet_1>) in Figure 3. This forces the model to make an explicit and interpretable grounding decision within the CoT sequence.

c) \mathcal{T}_{nav} : The model generates the navigation sequence “The navigation action: waypoint <waypoint>”, The special token <waypoint> is followed by the word “waypoint” and selects a waypoint from the candidate waypoints. The agent can move to this selected waypoint through the action controller.

d) $\mathcal{T}_{\text{answer}}$: A sequence of language tokens for internal monologue, question answering, or status description.

This formulation is not a simple chain-of-text. It is a multimodal chain-of-thought, where language reasoning ($\mathcal{T}_{\text{plan}}$) is directly followed by an explicit 3D grounding action ($\mathcal{T}_{\text{ground}}$) and a navigation action (\mathcal{T}_{nav}) within one autoregressive pass.

Grounding within 3D Tokens. The 3D-VLM first outputs a latent <target> token, which is passed through an MLP-based grounding_head(\cdot). We then compute dot-product similarities between the resulting feature and all 3D tokens from projector($\mathcal{M}_t \oplus \mathcal{P}_t$), and a special <grounding_none> token. The token with the highest similarity is selected as the grounded target and input into 3D-VLM for the subsequent autoregressive process.

Navigation within Candidate Waypoints. Similar to the grounding process, the latent <waypoint> token is first passed through an MLP-based navigation_head(\cdot). We then compute dot-product similarities between the resulting feature and all candidate waypoint embeddings from projector($\mathcal{P}_{\text{wayp}}$), and a special <navigation_stop> token. The candidate waypoint embedding with the highest similarity is selected as the next movement target, with <stop> indicating that the destination has been reached. Note that the model does not output <stop> for the subgoals within the sub-instruction from planning. Instead, after selecting the optimal next <waypoint>, it outputs the text tokens “reached the subgoal” to identify the completion

progress of the sub-instruction.

CoT Memory Feedback for Dynamic Replanning[†]. The *dynamic* nature of the 3D CoT is enabled by the memory feedback loop shown in Figures 2 and 3. Instead of discarding the generated sequence \mathcal{S}_t , we parse its components to update the historical CoT Memory for the next timestep:

$$\mathcal{C}_t = \text{Concat}(\mathcal{C}_{t-1}, \text{Parse}(\mathcal{S}_t)), \quad (2)$$

where $\text{Parse}(\mathcal{S}_t) = (\text{Parse}(\mathcal{T}_{\text{plan}}), \text{Parse}(\mathcal{T}_{\text{ground}}), \text{Parse}(\mathcal{T}_{\text{nav}}))$. Specifically, $\text{Parse}(\mathcal{T}_{\text{plan}})$ records the completed sub-instruction, $\text{Parse}(\mathcal{T}_{\text{ground}})$ records the grounded target token and position, and $\text{Parse}(\mathcal{T}_{\text{nav}})$ records the previously traversed waypoint position. \mathcal{C}_t is fed back into the 3D-VLM for the next decision-making step, as shown in Figure 3.

This mechanism makes the agent explicitly stateful and enables online re-planning, which directly addresses the “no dynamic replan” failure mode of static and multi-stage modular systems (*cf.* Figure 1). At each step, our D3D-VLP is forced to re-read its own history of previous plans, grounded targets, and executed trajectories in the input context. When a sub-instruction cannot be satisfied, *e.g.* when the target cannot be grounded, navigation becomes blocked, or the current plan stalls, the 3D-VLM can interpret these failure signals in \mathcal{C}_t and autoregressively propose a revised plan \mathcal{S}_{t+1} . This closed-loop design turns planning into a self-correcting process instead of a one-shot prediction.

3.3. Synergistic Fragmented Supervision

Training our D3D-VLP model with 3D CoT to achieve unified planning, grounding, and navigation remains a highly challenging task due to data scarcity and training difficulty. To address these challenges, we introduce ***Synergistic Learning from Fragmented Supervision*** (SLFS), which leverages a large-scale but fragmented 3D CoT dataset together with a masked autoregressive objective such that each partially annotated sample still contributes to joint learning of planning, grounding, and navigation.

Table 1. Composition of sample annotations in our constructed 3D CoT dataset. The fully annotated gold data is about 175K, and the partially annotated data is about 9.9M.

Data Type	Planning	Grounding	Navigation	# Samples
1	✓	✓	✓	175K
2	✓	✓	✗	161K
3	✓	✗	✓	14K
4	✗	✓	✓	5.8M
5	✗	✓	✗	2.3M
6	✗	✗	✓	1.6M

3D CoT Dataset. Collecting a massive dataset (*e.g.* 10M+ samples) with high-quality ground-truth for all 3D-CoT components ($\mathcal{T}_{\text{plan}}, \mathcal{T}_{\text{ground}}, \mathcal{T}_{\text{nav}}$) over every sample is economically infeasible. Instead, we construct a large-scale hybrid dataset of 10 million samples by aggregating data

from multiple heterogeneous sources. As summarized in Table 1, this dataset is fragmented. It contains a small subset of fully annotated *gold* samples (*e.g.* 175K), and large amounts of partially annotated data such as 1.6 million samples that only provide navigation annotations.

The ***planning annotations*** (data type 1,2,3) are mainly from SG3D [70], Grounded 3D-LLM [11] and VLN-Trans [68]. For 3D grounding (data type 5), we primarily collect 3D instance-text pairs from SceneVerse [27], MM-Scan [40], PQ3D [78], and Grounded 3D-LLM [11].

For ***open-vocabulary object grounding and navigation*** (data type 4), we use annotations in HM3D [45, 60] and MP3D [4] scenes from the above grounding datasets that support the Habitat simulator [42, 46]. We further integrate data from HSSD (Habitat) [28], ProcTHOR-10K (Habitat) [15, 28], and ProcTHOR-Objaverse (AI2-THOR) [16, 30]. For ***vision-and-language navigation*** (data type 6), we mainly adapt data from R2R-CE [31], REVERIE-CE [43, 56], SRDF [54], and NavRAG [57] to the Habitat simulator [42, 46].

The 3D scenes for above annotations include posed RGB-D videos from real environments such as ScanNet [14], 3RScan [49], and ARKitScenes [3]; real scans such as HM3D [45] and MP3D [4]; as well as synthetic scenes including HSSD [28], ProcTHOR-10K [15], and ProcTHOR-Objaverse [17].

Masked Autoregressive Loss. The SLFS mechanism is implemented at the loss-computation level. The D3D-VLP always generates the full sequence prediction $\mathcal{S}_{\text{pred}} = (\mathcal{T}_{\text{plan}}^{\text{pred}}, \mathcal{T}_{\text{ground}}^{\text{pred}}, \mathcal{T}_{\text{nav}}^{\text{pred}}, \mathcal{T}_{\text{answer}})$ for every sample in a batch. If the annotation for a CoT component is available, the corresponding multimodal tokens from the annotation are directly concatenated to the existing input tokens. If no annotation is available, the tokens for that CoT component are generated autoregressively, and these tokens are masked out during the cross-entropy loss computation.

For each sample i in the batch, we construct a ground-truth target sequence $\mathcal{S}_{\text{gt},i}$. Any missing annotation token (*e.g.* $\mathcal{T}_{\text{plan}}$ for a navigation-only sample) is populated with a special `<mask>` token in $\mathcal{S}_{\text{gt},i}$.

The total loss \mathcal{L}_{CoT} is then computed using a standard autoregressive cross-entropy loss, which is masked to ignore the `<mask>` tokens:

$$\mathcal{L}_{\text{CoT}} = \sum_{i \in \text{Batch}} \sum_{k \in \text{CoT}} \mathcal{H}_{i,k} \cdot \mathcal{L}_k(\mathcal{S}_{\text{pred},i}, \mathcal{S}_{\text{gt},i}) \quad (3)$$

where $\mathcal{H}_{i,k}$ is an indicator mask that is 1 if sample i has a valid annotation for CoT component k , and 0 otherwise.

This strategy enables synergistic learning across different data types:

Gold Data. These are the fully annotated samples, where all masks ($\mathcal{H}_{i,\text{plan}}, \mathcal{H}_{i,\text{ground}}, \dots$) are set to 1. The model

receives explicit end-to-end supervision over the entire CoT sequence. These samples act as *semantic anchors* to guide the model into aligning its internal representations with the correct language, grounding, and action tokens, *e.g.* “Go to the kitchen and take the bread to the living room table.”.

Partially Annotated Data. Using navigation-only data as an example, where only $\mathcal{H}_{i,\text{nav}} = 1$. The loss \mathcal{L}_{nav} is computed solely on $\mathcal{T}_{\text{nav}}^{\text{pred}}$. However, during the autoregressive forward pass, $\mathcal{T}_{\text{nav}}^{\text{pred}}$ is *conditioned on* the internally generated $\mathcal{T}_{\text{plan}}^{\text{pred}}$ and $\mathcal{T}_{\text{ground}}^{\text{pred}}$ of the model. As a result, the gradient from \mathcal{L}_{nav} back-propagates through the shared 3D-VLM and implicitly supervises the planning and grounding modules.

4. Experiments

4.1. Experimental Setup

Benchmarks. We evaluate D3D-VLP on a diverse suite of five challenging benchmarks:

1-3) Vision-and-Language Navigation (VLN). We use **R2R-CE** [2, 31], **REVERIE-CE** [43, 56], and **NavRAG-CE** [56, 57]. These tasks evaluate the ability of the agent to follow natural language instructions that ranges from step-by-step directions (R2R-CE) to coarse-grained destination descriptions (REVERIE-CE) and complex user-demand instructions (NavRAG-CE).

4) Object-Goal Navigation (OVON). We use **HM3D-OVON** [62] to assess the ability of the agent in navigating to open-vocabulary object categories in unseen large-scale environments.

5) Task-Oriented Sequential Grounding and Navigation (SG3D). We utilize the **SG3D** [70] benchmark, a highly challenging task requiring the agent to interpret a multi-step plan (*e.g.* “Make coffee”) and sequentially navigate to and ground context-dependent targets (*e.g.* “find a cup”, “go back to the other table”). Our setting is more challenging than the original benchmark which uses full scene since we require online grounding during navigation. Due to the infeasibility of exactly reproducing the ground-truth plan, we follow the original SG3D setting during evaluation that provides the ground-truth planning text as model input.

Evaluation Metrics. We evaluate our model using standard navigation metrics and stricter sequential grounding metrics as follows:

Navigation Benchmarks. For R2R-CE, REVERIE-CE, NavRAG-CE, HM3D-OVON, and SG3D Navigation, we report the standard metrics: Navigation Error (NE), Success Rate (SR), Oracle Success Rate (OSR), Success weighted by Path Length (SPL), step-Navigation Success Rate (s-SR), and task-Navigation Success Rate (s-SR).

Grounding Benchmarks. For the SG3D Grounding task, we introduce two stringent metrics:

- i. **s-ACC (step-Accuracy):** A single step is successful *only if* the agent successfully navigates to the correct target *and* correctly grounds the target, *i.e.* the point in the ground-truth instance point cloud that is closest to the grounded 3D token belongs to the target instance. This is much more challenging than the standard navigation-only step-SR.
- ii. **t-ACC (task-Accuracy):** A task is successful *only if* all navigation and grounding actions for *every step* in the sequence are correct.

Implementation Details. We next outline the key architectural choices and training setup of our D3D-VLP:

Model Architecture. Our D3D-VLP utilizes the Dynam3D Encoder [56] as the 3D perception backbone. This module processes streaming posed RGB-D images to maintain the multi-level 3D memory that comprises patch-level feature field [53], instance tokens $\mathcal{M}_{\text{inst}}$, zone tokens $\mathcal{M}_{\text{zone}}$, *etc.* The core reasoning module is a 3D-VLM based on a pre-trained NVILA-Lite-2B model [38]. The action space is defined by a waypoint predictor, which generates navigable candidates from panoramic patch tokens.

Training. The model is trained using our Synergistic Learning from Fragmented Supervision (SLFS) strategy (*cf.* Section 3.3) with our large-scale hybrid dataset of 10M samples in Table 1. The model is trained with the masked autoregressive cross-entropy loss for 100K episodes (\sim 14 days) on 4 RTX 6000 Ada GPUs with total batch size 8. Due to *limited computational resources*, we cannot use all available data for training. As shown in Table 1, we sample data of types 1, 2, and 3; types 4 and 5; and type 6 with approximately a 1:1:1 probability during training. All samples within the same batch are kept consistent in terms of data type, and the samples containing navigation tasks are trained online on the simulators [30, 46] with a DAgger augmentation strategy [1, 9].

4.2. Comparison with State-of-the-Art Methods

Table 2 shows the comparison results of our D3D-VLP with other existing methods on various embodied navigation benchmarks.

VLN Performance (R2R-CE, REVERIE-CE, NavRAG-CE). Our D3D-VLP establishes a new state-of-the-art across all end-to-end (E2E) models and modular systems on three VLN benchmarks. On the widely-used R2R-CE benchmark, our D3D-VLP sets a new SOTA with 61.3% SR and 56.1% SPL. This is a substantial improvement over prior end-to-end models, including StreamVLN [59] (+4.4% SR, +4.2% SPL) and NavFoM [66] (+5.1% SR, +4.9% SPL), and also surpasses the strongest modular system, InternVLA-N1 [13] (+3.1% SR, +2.1% SPL).

A critical comparison is against the perception baseline Dynam3D [56]. The sophisticated reasoning architecture

Table 2. Evaluation of embodied navigation benchmarks with monocular camera, * denotes zero-shot method.

Methods	System Type	R2R-CE				REVERIE-CE				NavRAG-CE				HM3D-OVON	
		NE↓	OSR↑	SR↑	SPL↑	NE↓	OSR↑	SR↑	SPL↑	NE↓	OSR↑	SR↑	SPL↑	SR↑	SPL↑
CM ² [20]	E2E	7.02	41.5	34.3	27.6	-	-	-	-	-	-	-	-	-	-
WS-MGMap [8]	E2E	6.28	47.6	38.9	34.3	-	-	-	-	-	-	-	-	-	-
InstructNav* [39]	Modular w/ CoT	6.89	-	31.0	24.0	7.44	31.5	25.2	19.1	9.83	24.1	17.4	10.9	-	-
CA-Nav* [7]	Modular	7.58	48.0	25.3	10.8	-	-	-	-	-	-	-	-	-	-
AO-Planner* [6]	Modular w/ CoT	6.95	38.3	25.5	16.6	-	-	-	-	-	-	-	-	-	-
DreamNav* [52]	Modular w/ CoT	7.06	41.0	32.8	29.0	-	-	-	-	-	-	-	-	-	-
VLFM* [61]	Modular	-	-	-	-	-	-	-	-	-	-	-	-	35.2	19.6
DAgRL+OD* [62]	Modular	-	-	-	-	-	-	-	-	-	-	-	-	37.1	19.8
MTU3D [79]	E2E	-	-	-	-	-	-	-	-	-	-	-	-	40.8	12.1
VLN-3DF [55]	E2E	5.95	55.8	44.9	30.4	-	-	-	-	-	-	-	-	-	-
g3D-LF [53]	E2E	5.70	59.5	47.2	34.6	6.50	41.6	34.4	23.8	8.85	31.8	21.4	13.5	-	-
NaVid [65]	E2E	5.47	49.1	37.4	35.9	6.74	36.3	26.6	20.8	9.35	29.6	19.4	13.9	-	-
MapNav [67]	Modular w/ CoT	4.93	53.0	39.7	37.2	-	-	-	-	-	-	-	-	-	-
Uni-NaVid [64]	E2E	5.58	53.3	47.0	42.7	-	-	-	-	-	-	-	-	39.5	19.8
NaVILA [12]	E2E	5.22	62.5	54.0	49.0	-	-	-	-	-	-	-	-	-	-
Aux-Think [50]	E2E	5.88	54.9	49.7	41.7	-	-	-	-	-	-	-	-	-	-
Dynam3D [56]	E2E	5.34	62.1	52.9	45.7	6.22	48.9	40.1	28.5	8.12	38.4	24.7	18.8	42.7	22.4
MonoDream [51]	E2E	5.45	61.5	55.8	49.1	-	-	-	-	-	-	-	-	-	-
StreamVNL [59]	E2E	4.98	64.2	56.9	51.9	-	-	-	-	-	-	-	-	-	-
NavFoM (S.RGB) [66]	E2E	5.01	64.9	56.2	51.2	-	-	-	-	-	-	-	-	43.6	31.3
InternVLA-N1 [13]	Modular	4.83	63.3	58.2	54.0	-	-	-	-	-	-	-	-	-	-
D3D-VLP (Ours)	E2E w/ CoT	4.73	67.2	61.3	56.1	5.36	56.9	47.5	34.7	7.57	45.3	31.1	23.9	47.3	30.4

Table 3. Evaluation of task-oriented sequential grounding and navigation task on SG3D-Nav [70] benchmark.

Methods	System Type	Navigation			Grounding	
		s-SR	t-SR	SPL	s-ACC	t-ACC
VideoAgent [18, 70]	Modular	14.7	3.8	10.2	-	-
SenseAct-NN [29, 70]	E2E	12.1	7.7	10.1	-	-
MTU3D [79]	E2E	23.8	8.0	16.5	-	-
Dynam3D-VisTA [56, 77]	Modular	26.4	9.3	15.4	21.4	4.2
D3D-VLP (Ours)	E2E w/ CoT	33.7	13.8	21.6	28.3	9.3

of our D3D-VLP provides a substantial boost of +8.4% SR and +10.4% SPL over the Dynam3D baseline. This result strongly suggests that our 3D CoT and unified architecture are the main contributors to the SOTA performance, and not merely from the strong 3D perception backbone.

ObjectNav Performance (HM3D-OVON). On the challenging open-vocabulary object navigation task, our D3D-VLP again achieves a new SOTA result with 47.3% SR and 30.4% SPL. This outperforms both the strongest E2E model, NavFoM (43.6% SR, 31.3% SPL), and our baseline method, Dynam3D (42.7% SR, 22.4% SPL). This demonstrates that our unified grounding-and-navigation pipeline is highly effective for object-centric tasks, and not only for instruction-following VLN.

4.3. Long-Horizon Grounding and Planning

The SG3D benchmark is specifically designed to evaluate planning, grounding, and memory capabilities in long-horizon stateful tasks of an agent.

Table 3 shows that our D3D-VLP demonstrates clear superiority on this complex long-horizon benchmark. Particularly, our model achieves a step-level navigation SR of 33.7% that significantly outperforms the next-best modular baseline (Dynam3D-VisTA, 26.4% SR) and the SOTA E2E model (MTU3D, 23.8% SR).

The true challenge of SG3D lies in sequential consistency measured by task-level metrics (t-SR and t-ACC). The baselines show a massive drop-off from step-success to task-success. For example, the Dynam3D-VisTA modular baseline, which pairs the strong 3D perception and navigation baseline model [56] with a 3D grounding model [77] achieves a 21.4% s-ACC but only a 4.2% t-ACC. It means that although $\sim 21\%$ *individual steps* are correctly executed, only $\sim 4\%$ *full tasks* are completed. This confirms the hypothesis that modular memory-less systems cannot handle the contextual dependencies such as “go back to it” inherent in sequential planning.

In contrast, our D3D-VLP achieves a t-ACC of 9.3%, which is a **121% relative improvement** over the Dynam3D-VisTA baseline (4.2%). Similarly, our navigation t-SR of 13.8% shows a **72.5% relative improvement** over the SOTA MTU3D (8.0%) and a 48% improvement over Dynam3D-VisTA (9.3%).

This significant improvement in task-level metrics is direct evidence that our **Dynamic 3D CoT** (*cf.* Section 3.2) and **CoT Memory** (*cf.* Section 3.1) are effective. By feeding historical plans, grounded targets, and trajectories back into the VLM, our D3D-VLP maintains state, resolves temporal ambiguities, and possesses replanning capabilities that are absent in both E2E and static modular systems.

4.4. Ablation Studies

Table 4. Ablation study on components and training data.

Settings	Training data	R2R-CE Nav.			SG3D Grounding	
		OSR	SR	SPL	s-ACC	t-ACC
All pipeline	All data	67.2	61.3	56.1	28.3	9.3
All pipeline	w/ T_{plan} (Type 1,2,3 in Tab. 1)	55.6	46.2	38.7	22.5	5.5
All pipeline	w/o T_{plan} (Type 4,5,6 in Tab. 1)	67.8	60.8	55.4	24.3	5.3
w/o CoT Memory	All data	65.7	56.5	48.7	19.4	4.1
Text-based actions	All data	66.3	56.4	48.8	27.8	8.6

To validate the design of our D3D-VLP, we conduct a thorough ablation study in Table 4 on the R2R-CE and SG3D benchmarks. We validate and analyze the *three core contributions* of our work:

1. **Synergistic Learning (SLFS) and Training Data.** Rows 2 and 3 of Table 4 analyze our SLFS strategy. Training *only* on samples with planning annotations (w/ $\mathcal{T}_{\text{plan}}$, types 1–3 in Table 1) leads to a large performance drop (SR 61.3% → 46.2% on R2R-CE; t-ACC 9.3% → 5.5% on SG3D), which confirms that high-quality fully annotated data alone is too scarce to train a robust agent. The ablation also reveals two complementary roles of SLFS: 1) SLFS enables the model to exploit massive partially annotated data (w/o $\mathcal{T}_{\text{plan}}$, types 4–6) to recover strong navigation performance (60.8% SR on R2R-CE, close to 61.3% with all data). 2) The small set of gold-standard planning data (w/ $\mathcal{T}_{\text{plan}}$) remains crucial for complex planning, where SLFS effectively leverages it to boost SG3D t-ACC from 5.3% to 9.3%.
2. **Dynamic 3D CoT (CoT Memory).** Row 4 (w/o CoT Memory) of Table 4 ablates the core of our Dynamic 3D CoT, which feeds historical plans, groundings, and trajectories back into the VLM. Removing this memory feedback loop causes a clear performance drop on the standard R2R-CE task (SR 61.3% → 56.5%). The SG3D Grounding results further provide the strongest evidence for our central claim that CoT Memory is the critical mechanism for long-horizon sequential tasks. Without it, the agent degenerates from a planning and stateful controller into a reactive and memory-less one, and the task-level accuracy t-ACC collapses from 9.3% to 4.1%.
3. **Unified 3D Spatial Embedding for Waypoint-based Action Space.** Row 5 of Table 4 shows replacing the waypoint-based action space with direct text-based actions such as “turn left 30 degrees” and “move forward 1.5 meters” leads to a substantial drop in navigation performance on R2R-CE. This suggests that the waypoint-based action space exploits the 3D reasoning capabilities of our D3D-VLP more effectively by operating within a unified 3D spatial embedding space from Section 3.1.

4.5. Real-World Mobile Manipulation Experiments

Table 5. Evaluation of real-world mobile manipulation task.

Methods	Nav.	Grounding & Grasp	Place	Task
OK-Robot [37]	11/32	4/16	3/16	0/10
DynaMem [36]	13/32	6/16	4/16	0/10
Dynam3D+OWLv2 [41, 56]	21/32	9/16	7/16	1/10
D3D-VLP (Ours)	23/32	12/16	11/16	3/10

To validate the real-world generalization capability of our D3D-VLP, we conduct real-world mobile manipulation experiments in Table 5. This task consists of sub-tasks including navigation, grounding and grasping the target, and

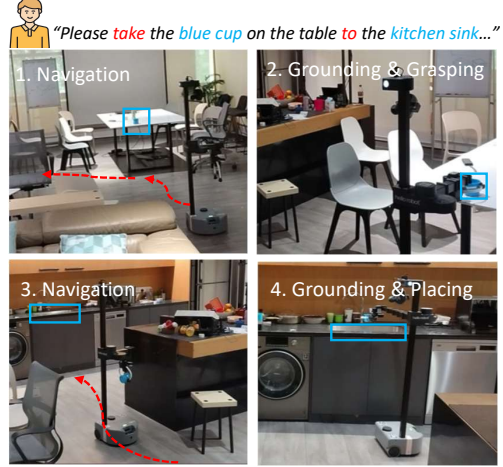


Figure 4. A demonstration of real-world mobile manipulation task.

then placing it at a specified location. For example: “Please take the blue cup on the table to the kitchen sink, then bring the red cup next to the sink to this table.” For a fair comparison, all methods use Hello Robot Stretch 3 with the AnyGrasp model [19] for object grasping and placing. We design 10 task samples with each comprising several sub-tasks. Our D3D-VLP fully completed 3 tasks, and significantly outperforming other baseline methods. This demonstrates its generalization ability on real-world long-horizon tasks. More visualizations are provided in the appendix.

5. Conclusion

This paper introduce D3D-VLP, a model that resolves the trade-off between opaque end-to-end and disjunct modular systems in embodied AI. Our core innovation is the Dynamic 3D Chain-of-Thought (3D CoT), which serves as the core engine for task planning by unifying multi-step planning, 3D grounding, and navigation within a single autoregressive 3D-VLM. This is powered by a CoT Memory feedback loop that is critical for stateful and dynamic replanning. To overcome data scarcity, we propose the Synergistic Learning from Fragmented Supervision (SLFS) strategy for effective training on a large-scale hybrid dataset. Our D3D-VLP demonstrates a significant step forward in the construction of high-performance embodied agents.

Limitations. Our current SLFS leverages implicit gradient signals to guide the CoT pipeline on unlabeled data, while its autoregressive CoT generation exhibits limited exploratory behavior. Future work could incorporate Reinforcement Learning to further enhance this framework. By actively exploring the planning, grounding, and action spaces and optimizing against environmental rewards, RL may enable more adaptive reasoning policies and better exploit the potential of large-scale unlabeled data.

References

[1] Dong An, Hanqing Wang, Wenguan Wang, Zun Wang, Yan Huang, Keji He, and Liang Wang. Etpnav: Evolving topological planning for vision-language navigation in continuous environments. *IEEE Transactions on Pattern Analysis and Machine Intelligence*, 2024. 6

[2] Peter Anderson, Qi Wu, Damien Teney, Jake Bruce, Mark Johnson, Niko Sünderhauf, Ian Reid, Stephen Gould, and Anton Van Den Hengel. Vision-and-language navigation: Interpreting visually-grounded navigation instructions in real environments. In *Proceedings of the IEEE conference on computer vision and pattern recognition*, pages 3674–3683, 2018. 1, 6

[3] Gilad Baruch, Zhuoyuan Chen, Afshin Dehghan, Yuri Feigin, Peter Fu, Thomas Gebauer, Daniel Kurz, Tal Dimry, Brandon Joffe, Arik Schwartz, et al. Arkitscenes: A diverse real-world dataset for 3d indoor scene understanding using mobile rgb-d data. In *Thirty-fifth Conference on Neural Information Processing Systems Datasets and Benchmarks Track (Round 1)*. 5, 13

[4] Angel Chang, Angela Dai, Thomas Funkhouser, Maciej Halber, Matthias Nießner, Manolis Savva, Shuran Song, Andy Zeng, and Yinda Zhang. Matterport3d: Learning from rgb-d data in indoor environments. In *International Conference on 3D Vision (3DV)*, 2017. 5, 13

[5] Dave Zhenyu Chen, Angel X Chang, and Matthias Nießner. Scanrefer: 3d object localization in rgb-d scans using natural language. In *European conference on computer vision*, pages 202–221. Springer, 2020. 1

[6] Jiaqi Chen, Bingqian Lin, Xinmin Liu, Lin Ma, Xiaodan Liang, and Kwan-Yee K Wong. Affordances-oriented planning using foundation models for continuous vision-language navigation. In *Proceedings of the AAAI Conference on Artificial Intelligence*, pages 23568–23576, 2025. 1, 2, 7

[7] Kehan Chen, Dong An, Yan Huang, Rongtao Xu, Yifei Su, Yonggen Ling, Ian Reid, and Liang Wang. Constraint-aware zero-shot vision-language navigation in continuous environments. *IEEE Transactions on Pattern Analysis and Machine Intelligence*, 2025. 7

[8] Peihao Chen, Dongyu Ji, Kunyang Lin, Runhao Zeng, Thomas Li, Mingkui Tan, and Chuang Gan. Weakly-supervised multi-granularity map learning for vision-and-language navigation. *Advances in Neural Information Processing Systems*, 35:38149–38161, 2022. 7

[9] Shizhe Chen, Pierre-Louis Guhur, Makarand Tapaswi, Cordelia Schmid, and Ivan Laptev. Think global, act local: Dual-scale graph transformer for vision-and-language navigation. In *Proceedings of the IEEE/CVF Conference on Computer Vision and Pattern Recognition*, pages 16537–16547, 2022. 6

[10] Shizhe Chen, Pierre-Louis Guhur, Makarand Tapaswi, Cordelia Schmid, and Ivan Laptev. Language conditioned spatial relation reasoning for 3d object grounding. *NeurIPS*, 2022. 1, 2

[11] Yilun Chen, Shuai Yang, Haifeng Huang, Tai Wang, Ruiyuan Lyu, Runsen Xu, Dahua Lin, and Jiangmiao Pang. Grounded 3d-lm with referent tokens. *arXiv preprint arXiv:2405.10370*, 2024. 1, 5, 13

[12] An-Chieh Cheng, Yandong Ji, Zhaojing Yang, Xueyan Zou, Jan Kautz, Erdem Biyik, Hongxu Yin, Sifei Liu, and Xiaolong Wang. Navila: Legged robot vision-language-action model for navigation. In *RSS*, 2025. 1, 2, 7

[13] InternNav Contributors. InternNav: InternRobotics’ open platform for building generalized navigation foundation models. <https://github.com/InternRobotics/InternNav>, 2025. 2, 6, 7

[14] Angela Dai, Angel X Chang, Manolis Savva, Maciej Halber, Thomas Funkhouser, and Matthias Nießner. Scannet: Richly-annotated 3d reconstructions of indoor scenes. In *Proceedings of the IEEE conference on computer vision and pattern recognition*, pages 5828–5839, 2017. 5, 13

[15] Matt Deitke, Eli VanderBilt, Alvaro Herrasti, Luca Weihs, Jordi Salvador, Kiana Ehsani, Winson Han, Eric Kolve, Ali Farhadi, Aniruddha Kembhavi, and Roozbeh Mottaghi. ProcTHOR: Large-Scale Embodied AI Using Procedural Generation. In *NeurIPS*, 2022. Outstanding Paper Award. 5, 13

[16] Kiana Ehsani, Tanmay Gupta, Rose Hendrix, Jordi Salvador, Luca Weihs, Kuo-Hao Zeng, Kunal Pratap Singh, Yejin Kim, Winson Han, Alvaro Herrasti, et al. Spoc: Imitating shortest paths in simulation enables effective navigation and manipulation in the real world. In *Proceedings of the IEEE/CVF Conference on Computer Vision and Pattern Recognition*, pages 16238–16250, 2024. 5, 13

[17] Kiana Ehsani, Tanmay Gupta, Rose Hendrix, Jordi Salvador, Luca Weihs, Kuo-Hao Zeng, Kunal Pratap Singh, Yejin Kim, Winson Han, Alvaro Herrasti, et al. Spoc: Imitating shortest paths in simulation enables effective navigation and manipulation in the real world. In *CVPR*, pages 16238–16250, 2024. 5, 13

[18] Yue Fan, Xiaojian Ma, Rongpeng Su, Jun Guo, Ruijie Wu, Xi Chen, and Qing Li. Embodied videoagent: Persistent memory from egocentric videos and embodied sensors enables dynamic scene understanding. *arXiv preprint arXiv:2501.00358*, 2024. 7

[19] Hao-Shu Fang, Chenxi Wang, Hongjie Fang, Minghao Gou, Jirong Liu, Hengxu Yan, Wenhui Liu, Yichen Xie, and Cewu Lu. Anygrasp: Robust and efficient grasp perception in spatial and temporal domains. *IEEE Transactions on Robotics*, 39(5):3929–3945, 2023. 8

[20] Georgios Georgakis, Karl Schmeckpeper, Karan Wanchoo, Soham Dan, Eleni Miltakaki, Dan Roth, and Kostas Daniilidis. Cross-modal map learning for vision and language navigation. In *Proceedings of the IEEE/CVF Conference on Computer Vision and Pattern Recognition*, pages 15460–15470, 2022. 7

[21] Qiao Gu, Ali Kuwajerwala, Sacha Morin, Krishna Murthy Jatavallabhula, Bipasha Sen, Aditya Agarwal, Corban Rivera, William Paul, Kirsty Ellis, Rama Chellappa, et al. Conceptgraphs: Open-vocabulary 3d scene graphs for perception and planning. In *2024 IEEE International Conference on Robotics and Automation (ICRA)*, pages 5021–5028. IEEE, 2024. 2

[22] Yining Hong, Yilun Du, Chunru Lin, Josh Tenenbaum, and Chuang Gan. 3d concept grounding on neural fields. *NeurIPS*, 35:7769–7782, 2022. 1

[23] Yicong Hong, Zun Wang, Qi Wu, and Stephen Gould. Bridging the gap between learning in discrete and continuous environments for vision-and-language navigation. In *Proceedings of the IEEE/CVF Conference on Computer Vision and Pattern Recognition (CVPR)*, 2022. 3

[24] Yining Hong, Haoyu Zhen, Peihao Chen, Shuhong Zheng, Yilun Du, Zhenfang Chen, and Chuang Gan. 3d-llm: Injecting the 3d world into large language models. *NeurIPS*, 36: 20482–20494, 2023. 2

[25] Jiangyong Huang, Silong Yong, Xiaojian Ma, Xiongkun Linghu, Puhalo Li, Yan Wang, Qing Li, Song-Chun Zhu, Baoxiong Jia, and Siyuan Huang. An embodied generalist agent in 3d world. In *Proceedings of the International Conference on Machine Learning (ICML)*, 2024. 2

[26] Shijia Huang, Yilun Chen, Jiaya Jia, and Liwei Wang. Multi-view transformer for 3d visual grounding. In *CVPR*, 2022. 1

[27] Baoxiong Jia, Yixin Chen, Huangyue Yu, Yan Wang, Xuesong Niu, Tengyu Liu, Qing Li, and Siyuan Huang. Sceneverse: Scaling 3d vision-language learning for grounded scene understanding. In *European Conference on Computer Vision (ECCV)*, 2024. 2, 5, 13, 14

[28] Mukul Khanna, Yongsen Mao, Hanxiao Jiang, Sanjay Haresh, Brennan Shacklett, Dhruv Batra, Alexander Clegg, Eric Undersander, Angel X Chang, and Manolis Savva. Habitat synthetic scenes dataset (hssd-200): An analysis of 3d scene scale and realism tradeoffs for objectgoal navigation. In *Proceedings of the IEEE/CVF Conference on Computer Vision and Pattern Recognition*, pages 16384–16393, 2024. 5, 13

[29] Mukul Khanna, Ram Ramrakhya, Gunjan Chhablani, Sriram Yenamandra, Theophile Gervet, Matthew Chang, Zsolt Kira, Devendra Singh Chaplot, Dhruv Batra, and Roozbeh Mottaghi. Goat-bench: A benchmark for multi-modal lifelong navigation. In *Proceedings of the IEEE/CVF Conference on Computer Vision and Pattern Recognition*, pages 16373–16383, 2024. 7

[30] Eric Kolve, Roozbeh Mottaghi, Winson Han, Eli VanderBilt, Luca Weihs, Alvaro Herrasti, Matt Deitke, Kiana Ehsani, Daniel Gordon, Yuke Zhu, et al. Ai2-thor: An interactive 3d environment for visual ai. *arXiv preprint arXiv:1712.05474*, 2017. 5, 6, 13

[31] Jacob Krantz, Erik Wijmans, Arjun Majumdar, Dhruv Batra, and Stefan Lee. Beyond the nav-graph: Vision-and-language navigation in continuous environments. In *Computer Vision–ECCV 2020: 16th European Conference, Glasgow, UK, August 23–28, 2020, Proceedings, Part XXVIII 16*, pages 104–120. Springer, 2020. 1, 5, 6, 13

[32] Alexander Ku, Peter Anderson, Roma Patel, Eugene Ie, and Jason Baldridge. Room-Across-Room: Multilingual vision-and-language navigation with dense spatiotemporal grounding. In *Conference on Empirical Methods for Natural Language Processing (EMNLP)*, 2020. 1

[33] Seungjun Lee, Yuyang Zhao, and Gim Hee Lee. Segment any 3d object with language. *arXiv preprint arXiv:2404.02157*, 2024. 2

[34] Bingqian Lin, Yunshuang Nie, Ziming Wei, Jiaqi Chen, Shikui Ma, Jianhua Han, Hang Xu, Xiaojun Chang, and Xiaodan Liang. Navcot: Boosting llm-based vision-and-language navigation via learning disentangled reasoning. *arXiv preprint arXiv:2403.07376*, 2024. 2

[35] Xiongkun Linghu, Jiangyong Huang, Ziyu Zhu, Baoxiong Jia, and Siyuan Huang. Scenecot: Eliciting grounded chain-of-thought reasoning in 3d scenes. *arXiv e-prints*, pages arXiv–2510, 2025. 2

[36] Peiqi Liu, Zhanqiu Guo, Mohit Warke, Soumith Chintala, Chris Paxton, Nur Muhammad Mahi Shafiuallah, and Lerrel Pinto. Dynamem: Online dynamic spatio-semantic memory for open world mobile manipulation. In *CoRL 2024 Workshop on Mastering Robot Manipulation in a World of Abundant Data*, . 1, 8, 13

[37] Peiqi Liu, Yaswanth Orru, Jay Vakil, Chris Paxton, Nur Muhammad Mahi Shafiuallah, and Lerrel Pinto. Ok-robot: What really matters in integrating open-knowledge models for robotics. In *First Workshop on Vision-Language Models for Navigation and Manipulation at ICRA 2024*, . 1, 2, 8

[38] Zhijian Liu, Ligeng Zhu, Baifeng Shi, Zhuoyang Zhang, Yuming Lou, Shang Yang, Haocheng Xi, Shiyi Cao, Yuxian Gu, Dacheng Li, et al. Nvila: Efficient frontier visual language models. In *Proceedings of the Computer Vision and Pattern Recognition Conference*, pages 4122–4134, 2025. 4, 6

[39] Yuxing Long, Wenzhe Cai, Hongcheng Wang, Guanqi Zhan, and Hao Dong. Instructnav: Zero-shot system for generic instruction navigation in unexplored environment. In *8th Annual Conference on Robot Learning*, 2024. 1, 2, 7

[40] Ruiyuan Lyu, Tai Wang, Jingli Lin, Shuai Yang, Xiaohan Mao, Yilun Chen, Runsen Xu, Haifeng Huang, Chenming Zhu, Dahua Lin, and Jiangmiao Pang. Mmscan: A multi-modal 3d scene dataset with hierarchical grounded language annotations. In *arXiv*, 2024. 5, 13

[41] Matthias Minderer, Alexey Gritsenko, and Neil Houlsby. Scaling open-vocabulary object detection. *Advances in Neural Information Processing Systems*, 36:72983–73007, 2023. 8

[42] Xavi Puig, Eric Undersander, Andrew Szot, Mikael Dallaire Cote, Ruslan Partsey, Jimmy Yang, Ruta Desai, Alexander William Clegg, Michal Hlavac, Tiffany Min, Theo Gervet, Vladimír Vondruš, Vincent-Pierre Berges, John Turner, Oleksandr MakSYMets, Zsolt Kira, Minal Kalakrishnan, Jitendra Malik, Devendra Singh Chaplot, Unnat Jain, Dhruv Batra, Akshara Rai, and Roozbeh Mottaghi. Habitat 3.0: A co-habitat for humans, avatars and robots, 2023. 5, 13

[43] Yuankai Qi, Qi Wu, Peter Anderson, Xin Wang, William Yang Wang, Chunhua Shen, and Anton van den Hengel. Reverie: Remote embodied visual referring expression in real indoor environments. In *Proceedings of the IEEE/CVF Conference on Computer Vision and Pattern Recognition*, pages 9982–9991, 2020. 1, 5, 6, 13

[44] Zhangyang Qi, Zhixiong Zhang, Ye Fang, Jiaqi Wang, and Hengshuang Zhao. Gpt4scene: Understand 3d scenes

from videos with vision-language models. *arXiv preprint arXiv:2501.01428*, 2025. 2

[45] Santhosh Kumar Ramakrishnan, Aaron Gokaslan, Erik Wijmans, Oleksandr Maksymets, Alexander Clegg, John M Turner, Eric Undersander, Wojciech Galuba, Andrew Westbury, Angel X Chang, et al. Habitat-matterport 3d dataset (hm3d): 1000 large-scale 3d environments for embodied ai. In *Thirty-fifth Conference on Neural Information Processing Systems Datasets and Benchmarks Track (Round 2)*. 5, 13

[46] Manolis Savva, Abhishek Kadian, Oleksandr Maksymets, Yili Zhao, Erik Wijmans, Bhavana Jain, Julian Straub, Jia Liu, Vladlen Koltun, Jitendra Malik, et al. Habitat: A platform for embodied ai research. In *CVPR*, pages 9339–9347, 2019. 5, 6, 13

[47] Chan Hee Song, Jihyung Kil, Tai-Yu Pan, Brian M Sadler, Wei-Lun Chao, and Yu Su. One step at a time: Long-horizon vision-and-language navigation with milestones. In *Proceedings of the IEEE/CVF conference on computer vision and pattern recognition*, pages 15482–15491, 2022. 2

[48] Xinshuai Song, Weixing Chen, Yang Liu, Weikai Chen, Guanbin Li, and Liang Lin. Towards long-horizon vision-language navigation: Platform, benchmark and method. In *Proceedings of the Computer Vision and Pattern Recognition Conference*, pages 12078–12088, 2025. 2

[49] Johanna Wald, Armen Avetisyan, Nassir Navab, Federico Tombari, and Matthias Nießner. Rio: 3d object instance re-localization in changing indoor environments. In *ICCV*, 2019. 5, 13

[50] Shuo Wang, Yongcai Wang, Wanting Li, Xudong Cai, Yucheng Wang, Maiyue Chen, Kaihui Wang, Zhizhong Su, Deying Li, and Zhaoxin Fan. Aux-think: Exploring reasoning strategies for data-efficient vision-language navigation. *arXiv preprint arXiv:2505.11886*, 2025. 7

[51] Shuo Wang, Yongcai Wang, Wanting Li, Yucheng Wang, Maiyue Chen, Kaihui Wang, Zhizhong Su, Xudong Cai, Yeying Jin, Deying Li, et al. Monodream: Monocular vision-language navigation with panoramic dreaming. *arXiv preprint arXiv:2508.02549*, 2025. 7

[52] Yunheng Wang, Yuetong Fang, Taowen Wang, Yixiao Feng, Yawen Tan, Shuning Zhang, Peiran Liu, Yiding Ji, and Renjing Xu. Dreamnav: A trajectory-based imaginative framework for zero-shot vision-and-language navigation. *arXiv preprint arXiv:2509.11197*, 2025. 1, 2, 7

[53] Zihan Wang and Gim Hee Lee. g3d-lf: Generalizable 3d-language feature fields for embodied tasks. *arXiv preprint arXiv:2411.17030*, 2024. 3, 6, 7, 13, 14

[54] Zun Wang, Jialu Li, Yicong Hong, Songze Li, Kunchang Li, Shoubin Yu, Yi Wang, Yu Qiao, Yali Wang, Mohit Bansal, et al. Bootstrapping language-guided navigation learning with self-refining data flywheel. In *The Thirteenth International Conference on Learning Representations*. 5, 13

[55] Zihan Wang, Xiangyang Li, Jiahao Yang, Yeqi Liu, and Shuqiang Jiang. Sim-to-real transfer via 3d feature fields for vision-and-language navigation. In *8th Annual Conference on Robot Learning*, 2024. 7

[56] Zihan Wang, Seungjun Lee, and Gim Hee Lee. Dynam3d: Dynamic layered 3d tokens empower vlm for vision-and-language navigation. In *Advances in Neural Information Processing Systems*, 2025. 1, 2, 3, 4, 5, 6, 7, 8, 13

[57] Zihan Wang, Yaohui Zhu, Gim Hee Lee, and Yachun Fan. Navrag: Generating user demand instructions for embodied navigation through retrieval-augmented llm. *arXiv preprint arXiv:2502.11142*, 2025. 1, 5, 6, 13

[58] Jason Wei, Xuezhi Wang, Dale Schuurmans, Maarten Bosma, Fei Xia, Ed Chi, Quoc V Le, Denny Zhou, et al. Chain-of-thought prompting elicits reasoning in large language models. *Advances in neural information processing systems*, 35:24824–24837, 2022. 2

[59] Meng Wei, Chenyang Wan, Xiqian Yu, Tai Wang, Yuqiang Yang, Xiaohan Mao, Chennming Zhu, Wenzhe Cai, Hanqing Wang, Yilun Chen, et al. Streamvln: Streaming vision-and-language navigation via slowfast context modeling. *arXiv preprint arXiv:2507.05240*, 2025. 1, 2, 6, 7

[60] Karmesh Yadav, Ram Ramrakhya, Santhosh Kumar Ramakrishnan, Theo Gervet, John Turner, Aaron Gokaslan, Noah Maestre, Angel Xuan Chang, Dhruv Batra, Manolis Savva, et al. Habitat-matterport 3d semantics dataset. In *Proceedings of the IEEE/CVF Conference on Computer Vision and Pattern Recognition*, pages 4927–4936, 2023. 5, 13

[61] Naoki Yokoyama, Sehoon Ha, Dhruv Batra, Jiuguang Wang, and Bernadette Bucher. Vlfm: Vision-language frontier maps for zero-shot semantic navigation. In *2024 IEEE International Conference on Robotics and Automation (ICRA)*, pages 42–48. IEEE, 2024. 7

[62] Naoki Yokoyama, Ram Ramrakhya, Abhishek Das, Dhruv Batra, and Sehoon Ha. Hm3d-ovon: A dataset and benchmark for open-vocabulary object goal navigation. In *2024 IEEE/RSJ International Conference on Intelligent Robots and Systems (IROS)*, pages 5543–5550. IEEE, 2024. 1, 6, 7

[63] Michał Zawalski, William Chen, Karl Pertsch, Oier Mees, Chelsea Finn, and Sergey Levine. Robotic control via embodied chain-of-thought reasoning. In *8th Annual Conference on Robot Learning*. 2

[64] Jiazhao Zhang, Kunyu Wang, Shaoan Wang, Minghan Li, Haoran Liu, Songlin Wei, Zhongyuan Wang, Zhizheng Zhang, and He Wang. Uni-navid: A video-based vision-language-action model for unifying embodied navigation tasks. *arXiv preprint arXiv:2412.06224*, 2024. 1, 2, 7

[65] Jiazhao Zhang, Kunyu Wang, Rongtao Xu, Gengze Zhou, Yicong Hong, Xiaomeng Fang, Qi Wu, Zhizheng Zhang, and He Wang. Navid: Video-based vlm plans the next step for vision-and-language navigation. In *Proceedings of Robotics: Science and Systems (RSS)*, 2024. 1, 2, 7

[66] Jiazhao Zhang, Anqi Li, Yunpeng Qi, Minghan Li, Jiahang Liu, Shaoan Wang, Haoran Liu, Gengze Zhou, Yuze Wu, Xingxing Li, et al. Embodied navigation foundation model. *arXiv preprint arXiv:2509.12129*, 2025. 6, 7

[67] L Zhang, X Hao, Q Xu, Q Zhang, X Zhang, P Wang, J Zhang, Z Wang, S Zhang, and R MapNav Xu. A novel memory representation via annotated semantic maps for vlm-based vision-and-language navigation. *arXiv preprint arXiv:2502.13451*, 2025. 7

[68] Yue Zhang and Parisa Kordjamshidi. Vln-trans: Translator for the vision and language navigation agent. In *Proceedings*

of the 61st Annual Meeting of the Association for Computational Linguistics (Volume 1: Long Papers), pages 13219–13233, 2023. 5, 13

- [69] Yiming Zhang, ZeMing Gong, and Angel X Chang. Multi3drefrer: Grounding text description to multiple 3d objects. In *ICCV*, pages 15225–15236, 2023. 1
- [70] Zhuofan Zhang, Ziyu Zhu, Junhao Li, Pengxiang Li, Tianxu Wang, Tengyu Liu, Xiaojian Ma, Yixin Chen, Baoxiong Jia, Siyuan Huang, and Qing Li. Task-oriented sequential grounding and navigation in 3d scenes. *arXiv preprint arXiv:2408.04034*, 2024. 1, 2, 5, 6, 7, 13
- [71] Lichen Zhao, Daigang Cai, Jing Zhang, Lu Sheng, Dong Xu, Rui Zheng, Yinjie Zhao, Lipeng Wang, and Xibo Fan. Towards explainable 3d grounded visual question answering: A new benchmark and strong baseline. *IEEE Transactions on Circuits and Systems for Video Technology*, 2022. 1
- [72] Duo Zheng, Shijia Huang, and Liwei Wang. Video-3d llm: Learning position-aware video representation for 3d scene understanding. *arXiv preprint arXiv:2412.00493*, 2024. 2
- [73] Duo Zheng, Shijia Huang, Lin Zhao, Yiwu Zhong, and Liwei Wang. Towards learning a generalist model for embodied navigation. In *Proceedings of the IEEE/CVF Conference on Computer Vision and Pattern Recognition*, pages 13624–13634, 2024. 2
- [74] Duo Zheng, Shijia Huang, Yanyang Li, and Liwei Wang. Learning from videos for 3d world: Enhancing mllms with 3d vision geometry priors. *arXiv preprint arXiv:2505.24625*, 2025. 2
- [75] Gengze Zhou, Yicong Hong, Zun Wang, Xin Eric Wang, and Qi Wu. Navgpt-2: Unleashing navigational reasoning capability for large vision-language models. In *European Conference on Computer Vision*, pages 260–278. Springer, 2024. 2
- [76] Chenming Zhu, Tai Wang, Wenwei Zhang, Jiangmiao Pang, and Xihui Liu. Llava-3d: A simple yet effective pathway to empowering lmms with 3d-awareness. *arXiv preprint arXiv:2409.18125*, 2024. 1, 2
- [77] Ziyu Zhu, Xiaojian Ma, Yixin Chen, Zhidong Deng, Siyuan Huang, and Qing Li. 3d-vista: Pre-trained transformer for 3d vision and text alignment. In *ICCV*, pages 2911–2921, 2023. 2, 7
- [78] Ziyu Zhu, Zhuofan Zhang, Xiaojian Ma, Xuesong Niu, Yixin Chen, Baoxiong Jia, Zhidong Deng, Siyuan Huang, and Qing Li. Unifying 3d vision-language understanding via promptable queries. In *European Conference on Computer Vision*, pages 188–206. Springer, 2024. 1, 2, 5, 13
- [79] Ziyu Zhu, Xilin Wang, Yixuan Li, Zhuofan Zhang, Xiaojian Ma, Yixin Chen, Baoxiong Jia, Wei Liang, Qian Yu, Zhi-dong Deng, et al. Move to understand a 3d scene: Bridging visual grounding and exploration for efficient and versatile embodied navigation. In *Proceedings of the IEEE/CVF International Conference on Computer Vision*, pages 8120–8132, 2025. 7

A. Details of 3D CoT Dataset

Grounding Annotations. We collect large-scale 3D instance-text pairs (Figure 5) primarily from SceneVerse [27], MMScan [40], PQ3D [78], and Grounded 3D-LLM [11], as illustrated in Listing 3.

Navigation Annotations. We adapt instruction-following navigation data from R2R-CE [31], REVERIE-CE [43, 56], SRDF [54], and NavRAG [57] for the Habitat simulator environment [42, 46].

Grounding-Navigation Annotations. For open-vocabulary object grounding and navigation, we leverage instance-text annotations from HM3D [45, 60] and MP3D [4] that support the Habitat simulator [42, 46]. We further integrate synthetic data from HSSD [28], ProcTHOR-10K [15, 28], and ProcTHOR-Objaverse (AI2-THOR) [16, 30]. To generate trajectories for these instances:

- **Habitat Simulator:** For HM3D, MP3D, HSSD, and ProcTHOR-10K (Habitat), the simulator computes optimal trajectories based on the scene mesh, ensuring collision-free paths with minimal distance.
- **AI2-THOR Simulator:** For ProcTHOR-Objaverse (AI2-THOR), as the native simulator [30] lacks a sufficient ground-truth path computation function for our needs, we implemented an A* algorithm based on traversable BEV maps to generate shortest paths while avoiding obstacles.

Planning-Grounding-Navigation Annotations. These comprehensive samples are primarily sourced from SG3D [70] and Grounded 3D-LLM [11]. As shown in Listing 1, these annotations contain hierarchical instructions with multiple sub-goals. Each sub-goal specifies the target object category, its index in the instance point cloud (Figure 5), and the center coordinates for the instance.

Planning-Grounding Annotations. Scenes with planning annotations that are currently incompatible with the Habitat simulator, specifically ScanNet [14], 3RScan [49], and ARKitScenes [3], are utilized for planning and grounding tasks. While these samples lack navigational trajectories, they provide rich instance-level grounding and planning instructions.

Planning-Navigation Annotations. We incorporate data from VLN-Trans [68] (see Listing 2). In these samples, the sub-goal coordinates correspond to trajectory waypoints rather than specific object instances, focusing on path planning and navigation without explicit object grounding.

3D Scene Composition. The annotations described above span a wide range of environments, including posed RGB-D videos from real-world datasets (ScanNet [14], 3RScan [49], ARKitScenes [3]), high-quality real scans (HM3D [45], MP3D [4]), and synthetic scenes (HSSD [28], ProcTHOR-10K [15], ProcTHOR-Objaverse [17]).

Grounding Label Assignment. Unlike traditional 3D grounding tasks where all candidate objects are visible,

the target object may be unobserved (i.e., lacking corresponding 3D tokens) during our online training. In such cases, the grounding output is assigned to a special `<grounding_none>` token. When tokens corresponding to the target instance exist within the patch or instance tokens, we optimize the model using a multi-label cross-entropy loss, treating the target tokens as positive samples and the rest as negative. Following g3D-LF [53] and Dynam3D [56], a 3D token is assigned to an instance based on its nearest neighbor in the ground-truth instance point cloud (available in HM3D, MP3D, ScanNet, 3RScan, and ARKitScenes). For scenes lacking instance point cloud annotations (e.g., HSSD, ProcTHOR-10K, and ProcTHOR-Objaverse), we only consider patch tokens within a 0.2m radius of the target instance center as positive samples.

B. Details of Real-world Mobile Manipulation

We validate the effectiveness of our D3D-VLP in real-world scenarios using the Hello Robot Stretch 3 mobile manipulator. The robot is equipped with a head-mounted Intel RealSense D435i RGB-D camera, which captures streaming posed RGB-D images. These streams are processed in real-time by the Dynam3D Encoder [56] to incrementally construct and update the Multi-level 3D Memory, ensuring the agent maintains a persistent and structured 3D scene representation during exploration.

For inference, we deploy the model on a remote workstation equipped with an NVIDIA RTX 4090 GPU and 64GB of RAM. The workstation handles the computationally intensive 3D-VLM reasoning and Dynamic 3D CoT generation, communicating with the robot via a local area network (LAN) over WiFi. Our deployment framework is adapted from DynaMem [36], which we extended to support our waypoint-based action space and local obstacle avoidance. The experiments are conducted in a physical home-like environment comprising a living room, kitchen, meeting room, and office. Crucially, to strictly evaluate zero-shot generalization, none of the objects or scene layouts in this environment are included in the training dataset.

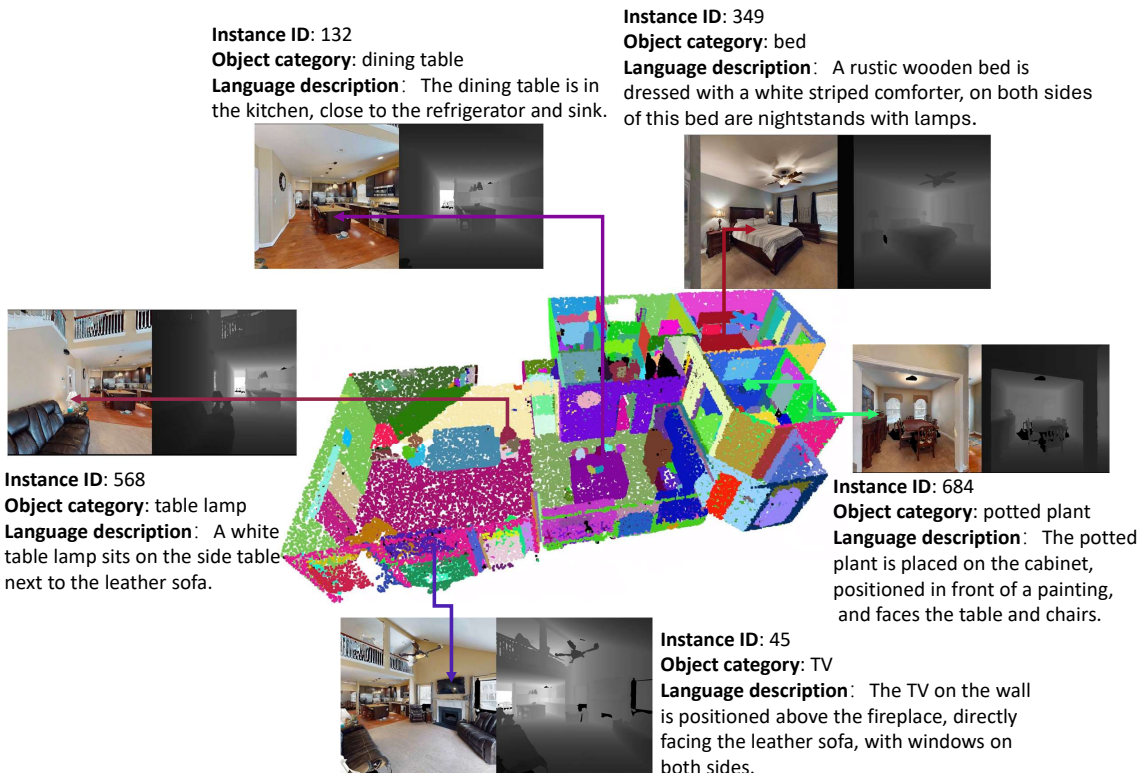


Figure 5. Demonstration of a 3D scene in the training data [27, 53]. Instance-level point clouds mark all instances with object categories and language descriptions.

Listing 1. Planning-Grounding-Navigation Annotation. An example showing the unified data structure and the corresponding prompt format.

```

1 // 1. JSON Annotation
2 {
3     "scene_id": "hm3d/00378-DqJKU7YU7dA",
4     "instruction": "Prepare for a shower.",
5     "planning": [
6         "1. Go to the shower containing a washcloth.",
7         "2. Turn on the water to adjust the temperature.",
8         "3. Take a towel from the rack stand to the left of the sink.",
9         "4. Hang the towel on the shower curtain rod right by the shower."
10    ],
11    "instance_id": [[797], [797], [230], [515]],
12    "instance_type": ["shower", "shower", "towel", "shower curtain rod"],
13    // Coordinates truncated for display
14    "instance_position": [
15        [-6.554, -28.336, 0.863],
16        [-6.554, -28.336, 0.863],
17        [-2.407, -14.418, 1.189],
18        [-3.649, -20.311, 0.981]
19    ]
20 }
21
22 // 2. Input Prompt Trace
23 <|im_start|>system\n You are a helpful assistant<|im_end|>\n
24 <|im_start|>user\n
25 <patch tokens>\n <instance tokens>\n <zone tokens>\n
26 The instruction: Prepare for a shower.\n
27 The history plans: 1. Go to the shower containing a washcloth.<shower_1>\n
28 The previous waypoints:<waypoint_4>,<waypoint_7>,<waypoint_9>,<waypoint_15>\n
29 The candidate waypoints: <waypoint_17><waypoint_18><waypoint_19>\n
30 Please give deep thinking plans. <|im_end|>\n<|im_start|>assistant\n
31 // 3. Output Trace
32 The next plans: 2. Turn on the water to adjust the temperature.\n
33 3. Take a towel from the rack stand to the left of the sink.\n
34 4. Hang the towel on the shower curtain rod right by the shower.\n
35 The grounded:target<shower_1>\n
36 The navigation action:waypoint<waypoint_19>reached the subgoal\n
37 <|im_end|>

```

Listing 2. Planning-Navigation Annotation. An example for vision-and-language navigation task with detailed step descriptions.

```
1 {
2     "scene_id": "mp3d/PX4nDJXEHrG",
3     "instruction": "Walk across patio into the house. Walk forward toward wall with stone tile. Walk past stone tile
4         wall on left side. Walk past stair case. Stop at entrance to kitchen area.",
5     "planning": [
6         "1. Walk across patio into the house.",
7         "2. Walk forward toward wall with stone tile.",
8         "3. Walk past stone tile wall on left side.",
9         "4. Walk past stair case.",
10        "5. Stop at entrance to kitchen area."
11    ],
12    "habitat_start_position": [-11.546, 0.115, 4.632],
13    "habitat_start_rotation": [0, 0.998, 0, -0.049],
14    "instance_id": [[-10000],[-10000],[-10000],[-10000],[-10000]],
15    "instance_type": [null,null,null,null,null],
16    "instance_position": [
17        [-11.559, -3.040, 0.115],
18        [-11.066, -1.661, 0.115],
19        [-12.035, 1.826, 0.115],
20        [-13.690, 4.130, 0.115],
21        [-13.619, 5.133, 0.115]
22    ]
23 }
```

Listing 3. Grounding-Navigation Annotation. An example for open-vocabulary object grounding and navigation task without explicit intermediate planning steps.

```
1 {
2     "scene_id": "hm3d/iigzGirtanx",
3     "instruction": "Please find the printer. The printer is next to the paper tray and is placed on desk.",
4     "planning": "",
5     "instance_id": [[96]],
6     "instance_type": ["printer"],
7     "instance_position": [
8         [6.704, 1.147, 2.792]
9     ]
10 }
11 }
```